PCCP

Accepted Manuscript

ROYAL SOCIETY OF CHEMISTRY

www.rsc.org/pccp

Single-layer graphene-assembled 3D porous carbon composite with PVA and Fe_3O_4 nano-fillers: an interface-mediated superior dielectric and EMI shielding performance

B.V. Bhaskara Rao[a], Prasad Yadav[c], Radhamanohar Aepuru[b], H.S. Panda*[b], Satishchandra Ogale*[c], S.N. Kale*[a]

[a]Department of Applied Physics, Defence Institute of Advanced Technology, Girinagar, Pune 411025, India.

[b]Department of Materials Engineering, Defence Institute of Advanced Technology, Girinagar, Pune 411025, India.

[c]National Chemical Laboratory, Homi Bhabha Road, Pashan, Pune 411008, India.

ABSTRACT: In this study, a novel composite of Fe_3O_4 nanofiller-decorated single-layer graphene-assembled porous carbon (SLGAPC) with polyvinyl alcohol (PVA) having flexibility and density of 0.75 g/cm^3 is explored for its dielectric and electromagnetic interference (EMI) response properties. The composite is prepared by solution casting method and its constituents are optimized as 15 wt% SLGAPC and 20 wt% Fe_3O_4 through a novel solvent relaxation nuclear magnetic resonance experiment. The PVA-SLGAPC-Fe_3O_4 composite shows high dielectric permittivity in the range of 1 Hz – 10 MHz, enhanced by a factor of 4 as compared to that of the PVA-SLGAPC composite, with a reduced loss by a factor of 2. The temperature dependent dielectric properties reveal the activation energy behaviour with reference to the glass transition temperature (80 ^{o}C) of PVA. The dielectric hysteresis with temperature cycle reveals a remnant polarization. The enhanced dielectric properties are suggested to be the result of improvement in the localized polarization of the integrated interface system (Maxwell−Wagner−Sillars (MWS) polarization) formed by the uniform adsorption of Fe_3O_4 on the surface of SLGAPC conjugated with PVA. The EMI shielding property of the composite with low thickness of 0.3 mm in the X-band (8.2 GHz - 12.4 GHz) shows very impressive shielding efficiency ~15 dB and specific shielding effectiveness of 20 dB/(g/cm^3); indicating the promising character of this material for flexible EMI shielding application.

KEYWORDS: three phase nanocomposite; single-layer-graphene-assembled porous carbon; Fe_3O_4 nanoparticles, Maxwell−Wagner−Sillars (MWS) relaxation; Interfacial polarization

INTRODUCTION

Carbon based materials are encountered in diverse forms and functions reflecting an interesting variety of sp^2/sp^3 bonding patterns, morphologies and properties. Their novel synthesis and applications have acquired great significance in recent times. Graphene, carbon nanotubes, activated carbon, fullerenes are a few forms of carbon which have been synthesised using many novel routes so as to manipulate their surface area, porosity, electron conductivity etc. in the interest of specific applications. Amongst the physical properties of interest to several applications, dielectric constant is a basic property that can singularly drive certain applications, and in most cases its value is required to be large. Various composites with different polymers have been studied thus far and dopants have also been incorporated to enhance this property, without compromising the other desired properties such as the mechanical, optical and electrical propeties.[1–3] The fillers chosen are nanosized which can improve the capacitive capability of the percolative polymer composite network and also alter the permittivity resulting in enhancement of their absorption capability.[4] Some examples of materials examined in this context are Carbon black/Graphene nano ribbon,[5, 6] graphene/graphene oxide (GO),[7–12] expanded graphite[13] and chemically modified graphene.[14] All these have been used to make polymer composites with a variety of polymers such as PVDF, PVA, and PMMA.[5-14]

When appropriate fillers are added to polymers or resins they show remarkable changes in dielectric constant and relaxation behaviour.[1, 5, 15-16] For example, G.S. Parries et. al.[16] have shown that epoxy resin loaded with Fe_3O_4 nanoparticles fillers show significant changes in the dielectric properties over frequency range of 5Hz-13MHz and temperature range from ambient to 140^{o}C. In PVA polymer, a composite with graphite has shown a dielectric constant value in the range of 7-13 and with graphitic oxide it has shown a value between 12-30.[7] The

variations, as documented, are due to the graphite / GO percentage variation in the PVA matrix. Pure PVA has been shown to give the dielectric constant value of ~ 10.[17-18] Though there have been various literature values of dielectric constants, with different combinations of polymer composites with various carbon-based materials, the values have been in the range of up to a maximum of ~ 50. Higher values are related to the density of available free electrons, local polarization, dipole moments formed and the bulk conductivity of the sample. With the advent of hierarchically porous materials and the growing interest in the electric double layer type ultra capacitor systems, the domain of dielectric theory of interface systems has matured considerably and hence new materials, their composites and additional dopant incorporation protocols are being intensely researched to achieve higher values of dielectric constants. These have natural benefits to a range of applications including an important defence application of electromagnetic shielding. A brief literature survey of different carbon dopants into PVA polymer giving different values of dielectric constants show that the value varies between 10 to 50 with around 5 wt/vol % ratio. [6,7 and 17]

In this manuscript, we have explored the use of a new form of carbon, namely single-layer graphene-assembled porous carbon (SLGAPC) synthesized using chemical route[19] for its dielectric response, in a composite form with polyvinyl alcohol (PVA). Additionally, iron oxide (Fe_3O_4) nanoparticles are used as fillers and impedance spectroscopy is used for dielectric studies. The loading of SLGAPC and Fe_3O_4 in the PVA matrix is optimized (15% of SLGAPC and 20% of Fe_3O_4, by weight) using time-domain solvent relaxation method and thermo gravimetric analysis. The dielectric measurements were made both in terms of frequency and temperature variation, and the results of PVA-SLGAPC-Fe_3O_4 composite have been compared with those on PVA- SLGAPC and pure PVA. Electromagnetic shielding studies are further done to envisage the properties of this composite as a potential EMI shield in the X-band (8.2 GHz -12.4 GHz).

The frequency dependent studies show that the real part of dielectric constant in PVA-SLGAPC- Fe_3O_4 is 4 times higher as compared to that of PVA- SLGAPC. The PVA-SLGAPC composite itself shows much higher values than the reported counterparts[7-12] and pure PVA[17]. Temperature dependent studies were performed in the same range of frequencies with temperature variation from -30 ^oC to 120 ^oC, for all the systems. A prominent change in the dielectric behaviour is noted at around the glass transition temperature of PVA (T_g ~ 80 ^oC =353 K).[18] There is a systematic rise in the dielectric constant value till T_g and the behaviour is seen to be altered above this temperature. The enhanced dielectric properties below Tg are suggested to be the result of improvement in the localized polarization of the integrated interface system (Maxwell−Wagner−Sillars (MWS) polarization) formed by the adsorption of Fe_3O_4 on the surface of SLGAPC conjugated with PVA. Further, the imaginary part of dielectric constant shows an improvement as well; with the composite having a loss factor decreased by 50% as compared the value for PVA- SLGAPC. The composite (in the form of the three phase system) was subjected to thermal cycle (30 ^oC-120 ^oC) at 1 KHz, which showed a hysteresis in the dielectric constant value of the composite. This confirms that there is a remnant polarization in the system, which can emanate from the localized and interfacial polarization. These results establish that PVA-SLGAPC-Fe_3O_4 can be a promising system for energy storage as well as for EMI applications. Its flexibility and self-supporting nature are added advantages. The EMI studies were then performed in the range of X-Band, which show a substantial improvement in the shielding efficiency of the three-phase system (15 dB) as compared to its counterparts (PVA-SLGAPC ~10 dB).

EXPERIMENTAL DETAILS

Materials and Methods: Poly (4-styrenesulfonic acid-co-maleic acid) sodium salt (PSSCMA) was obtained from Sigma Aldrich (20,000 $gmol^{-1}$). The magnetite (Fe_3O_4)

nanoparticles were prepared from precursor solutions containing iron nitrate ($Fe(NO_3)_3.9H_2O$) as a source of Fe^{3+} ion and iron sulphate ($FeSO_4.7H_2O$) as a source of Fe^{2+} ions, which was obtained from Thomas Baker Pvt. Limited, Mumbai. PVA with MW~ 145,000 was purchased from Sigma-Aldrich.

Synthesis of SLGAPC: The detailed procedure has been reported elsewhere.[19] In brief, for pyrolytic decomposition, the polymer PSSCMA was heat-treated in a furnace at 1000 ^oC for 4h in argon atmosphere. The product formed by pyrolysis was then washed and purified carefully with deionized water to remove inorganic by-products. The process was repeated until the pH of the water in which the carbon mass was dispersed became neutral. The carbon mass was then dried to obtain SLGAPC.

Synthesis of Fe_3O_4: The nano material samples of Fe_3O_4 (~ 11 nm) were prepared using reverse co-precipitation route, which is also described elsewhere.[20, 21] In brief, Fe_3O_4 nanoparticles were synthesized using reverse co-precipitation method. $FeSO_4.7H_2O$ and $Fe(NO_3)_3$ (1:2 molar ratio) were dissolved in 200 ml DDW. 30% ammonia (NH_4OH) solution was diluted by adding DDW (i.e., 3:2 ratio) and heated to 80 ^oC under continuous argon gas flow in a three-neck flask. The Fe-salt solution was added to ammonia solution under vigorous stirring and was further stirred vigorously for 30 min under argon gas flow, keeping the temperature constant at 80 ^oC and was then removed from the flask. The solution was rapidly cooled to room temperature using an ice bath and was then washed with DDW until the pH dropped down to 7. The black slurry was further dried for characterization.

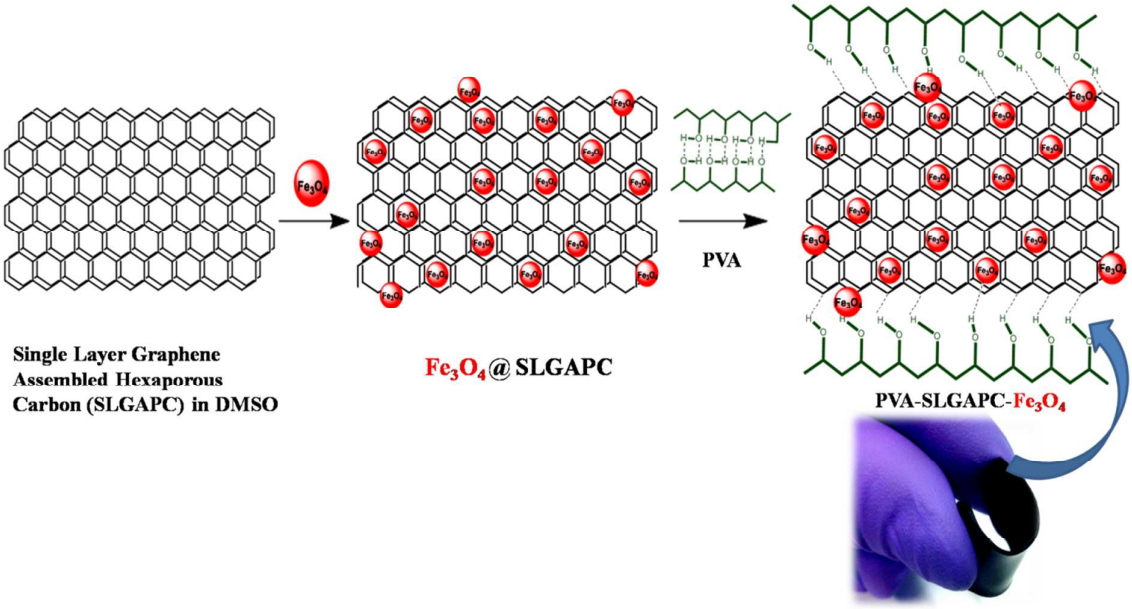

Figure 1: Schematic representation of PVA-SLGAPC- Fe_3O_4 three phase composite

Synthesis of PVA-SLGAPC-Fe_3O_4 composite: After due optimisation (as discussed in detail below), the loading percentages were fixed. The percentage of Fe_3O_4 and SLGAPC used in PVA matrix were 20% and 15%, respectively. SLGAPC of 0.3 g was well dispersed in 10 ml of DMSO under sonication for 30 minutes, then after 0.4 g of Fe_3O_4 nanoparticles were added to SLGAPC solution under continuous sonication for 30 more minutes. Simultaneously 1.3 g of PVA solution was prepared in 20 ml of deionised water at 80 ^oC under continuous stirring. There after Fe_3O_4 – SLGAPC solution was added to PVA solution and stirred for 2 hours. Finally the uniformly mixed solution of PVA-15%SLGAPC-20% Fe_3O_4 was poured onto acrylic sheets of desired shapes and dried in vacuum oven at 60^oC overnight to get films by solution casting method. For comparison, PVA- Fe_3O_4 and PVA-SLGAPC composite films were also prepared by the same method. Figure 1 shows the schematic representation of the composite formed. The flexibility obtained due to PVA polymer is also shown.

CHARACTERIZATION

Pure materials and composites are characterized using X-ray Diffraction (XRD, Bruker D8 advance equipped with Ni-filtered CuK_α radiation (λ=1.5418 Å) and operated at 45 kV), Field Emission Scanning electron microscopy (FE-SEM, CARL ZEISS'S ƩIGMAFESEM) and transmission electron microscopy (TEM, FEI tecnai). The composites were studied for loading and conjugation chemistry using thermo-gravimetric analyzer (TGA, PerkinElmer STA 6009) and Fourier transform infrared spectroscopy (FTIR, BRUKER Alpha ATR). Adsorption and stability studies were carried out using Acron surface area analyzer (XIGO nanotools) equipped with Acron Area Quant Software version 0.82, which worked on time domain nuclear magnetic Resonance (NMR). Dielectric studies were performed using Novacontrol Broadband dielectric spectrometer with Alpha-A analyzer interfaced to the sample cell equipped with temperature controller in the range of 1 Hz to 10 MHz over the temperature (-30^{o}C - 120^{o}C). EMI shielding property was measured by using PNA Network Analyzer N5222A ranging from 10 MHz - 26.5 GHz (Agilent).

RESULTS AND DISCUSSION

Optimisation of Filler loading and stability studies: In order to establish the fillers and the composite ratios in the PVA matrix, first we optimised the composition of the SLGAPC in PVA matrix by varying the SLGAPC percentage from 0 to 20 wt % and measuring the dielectric permittivity. As shown in Figure 2(a), the permittivity increases till 15 wt% and then it decreases thereafter, for 20 wt.%. Furthermore, the sample remains flexible till 15 wt%, after which the film breaks down due to its fragile nature. The insets of Fig. 2(a) show both these pictorial representations. Hence 15 wt% of SLGAPC was established as the optimised percentage in the PVA matrix, which was used for further studies. It is useful to note that the conductivity of the composite is also high at this percent composition, as is

shown in supporting information Figure S 1. The maximum adsorption limit study of Fe_3O_4 in SLGAPC was carried out by performing solvent relaxation nuclear magnetic resonance (NMR) experiment by measuring the specific relaxation rate enhancement R_{2sp}

$$\boldsymbol{R_{2sp} = \left({R_2}/{R_{2b}} - 1 \right)} \quad (1)$$

Where R_2 and R_{2b} were experimentally determined solvent relaxation rates of SLGAPC - Fe_3O_4 and bulk SLGAPC in DMSO respectively. The adsorption of Fe_3O_4 onto porous SLGAPC showed enhanced relaxation rate as compared to pure SLGAPC, which can be attributed to the change of specific surface relaxivity by the adsorbed Fe_3O_4 on SLGAPC.[22] Figure 2(b) shows saturation in relaxation rate enhancement R_{2sp}, which starts from 20 wt.% concentration of the Fe_3O_4 in SLGAPC. This occurs because of the inability of the excess Fe_3O_4 nanoparticles to load on SLGAPC.

Stability studies of Fe_3O_4, SLGAPC and SLGAPC-Fe_3O_4 fillers in PVA solution were carried out by measuring relaxation time as a function of time, where relaxation time of bound liquid has different relaxation rate from that of free liquid. The average spin-spin relaxation rate ($R_{n(av)}$, n=2 for spin-spin relaxation (T_2) method) is explained by the expression[22]

$$R_{n(av)} = P_s R_b + P_b R_f \quad (2)$$

where R_b is the relaxation rate constant of bound liquid with dispersed particles, R_f is the relaxation rate constant of free liquid, and P_b, P_s are the fractions of liquid in bulk phase and at the surface, respectively. The results in Figure 2(c) suggest that SLGAPC-Fe_3O_4 is more stable in PVA solution than pure SLGAPC by keeping relaxation time T_2 is constant with time. The increment in T_2 of SLGAPC is due to weak interaction between SLGAPC and PVA matrix solution leading to the instability of the composite.[22] Hence it is proposed that the adsorption of Fe_3O_4 on SLGAPC acts as an interface and stabilizes the SLGAPC in PVA solution due to strong interaction between the matrix and fillers. By these adsorption and

stability studies, it is practically useful to formulate composite films by solution casting method, where solvent evaporation is time dependent. These results are further substantiated in upcoming discussions.

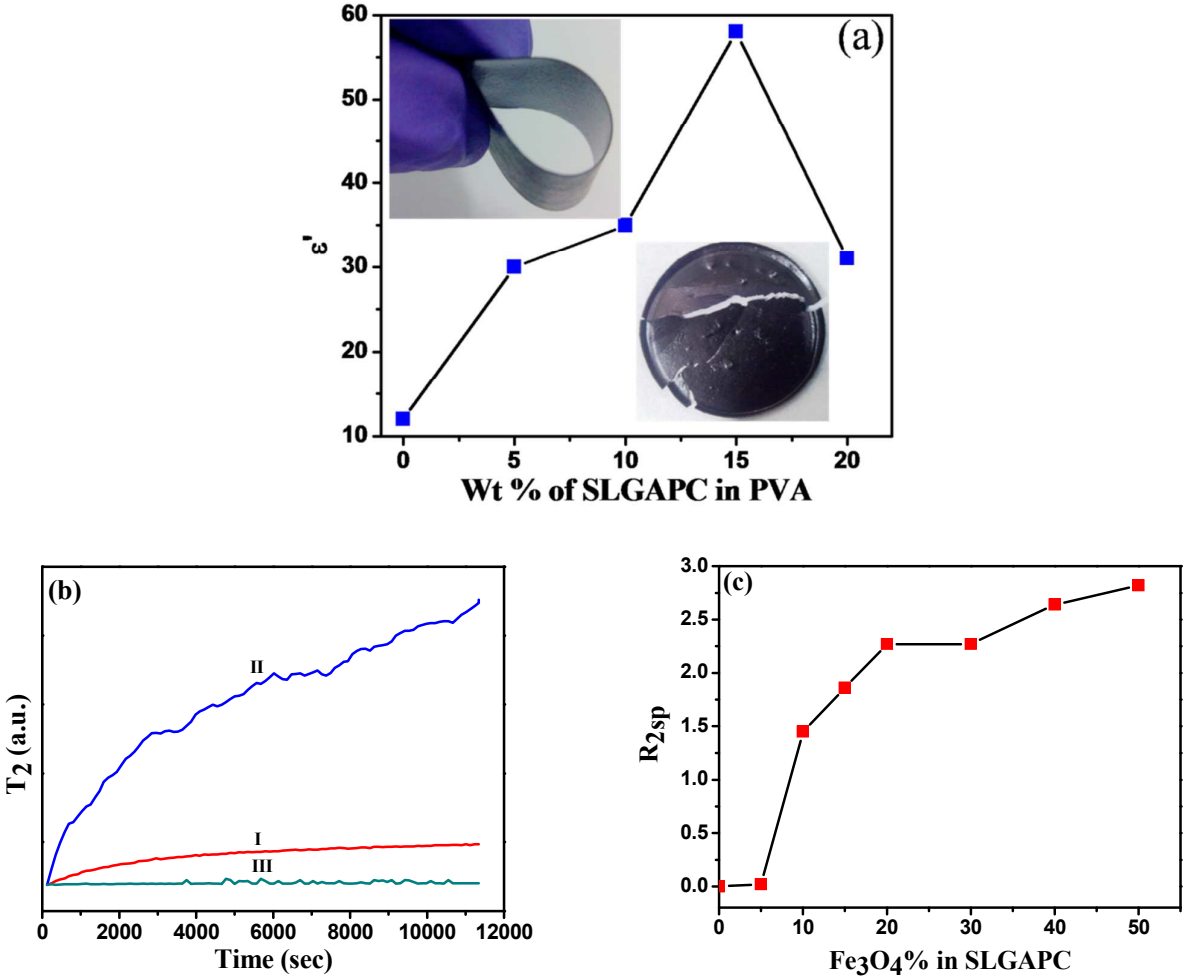

Figure 2 a) shows dielectric permittivity (ε') v.s. wt % of SLGAPC in PVA composites at 1.133 KHz. Inset shows brittleness of 20 wt% sample as well as flexibility of 15 wt% sample. (b) shows relaxation rate enhancements (R_{2SP}) of SLGAPC at various concentrations of Fe_3O_4 and (c) shows the stability studies of: I) PVA- Fe_3O_4, II) PVA-SLGAPC and III) PVA-SLGAPC- Fe_3O_4

XRD and TGA analysis: Figure 3(a) shows the XRD patterns of I) PVA, II) PVA- Fe_3O_4, III) PVA-SLGAPC and IV) PVA-SLGAPC- Fe_3O_4, respectively. The entire scans of SLGAPC and Fe_3O_4 nanoparticles systems are shown in the inset. Since PVA and SLGAPC were polymeric and carbon-based systems, the XRD signatures are quite broad and only a characteristic signature of PVA is seen at 19^o (plane (101)). Individual scan of Fe_3O_4, as shown in the inset did show the cubic phase of the nanomaterial, as checked through the standard data provided by JCPDS (Card No.89-0691). SLGAPC phase has already been reported by Yadav et al.[19] In the case of PVA-SLGAPC-Fe_3O_4 system the signature of iron oxide was seen at 2θ value of 35.49^o (corresponding to plane (311)).[23-24]

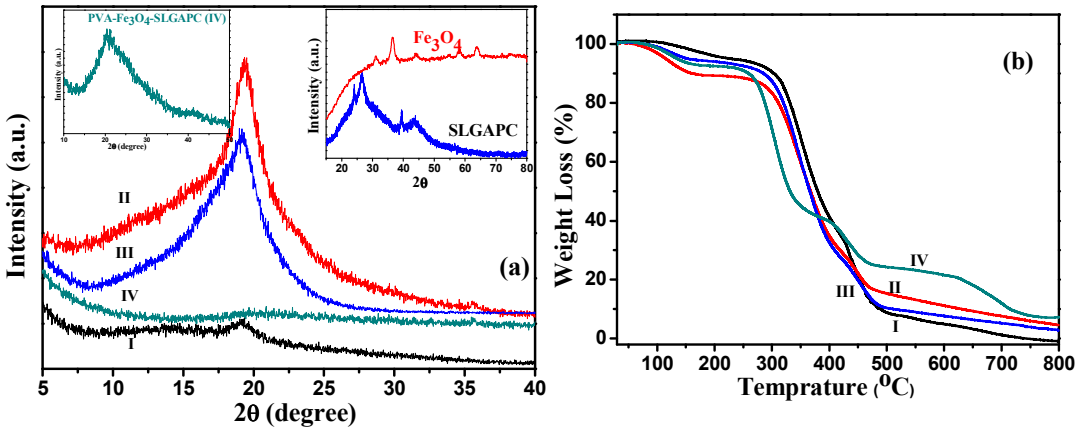

Figure 3: (a) X ray diffraction pattern of various samples. Right inset shows magnified XRD of sample IV and other inset shows XRD of individual fillers, (b) Thermo gravimetric analysis of I) PVA, II) PVA- Fe_3O_4, III) PVA-SLGAPC, IV) PVA-SLGAPC- Fe_3O_4 composites.

Figure 3 (b) shows TGA data of the samples, which were recorded in the temperature range 30-800 ºC at a heating rate of 20^{o}C/min under N_2 atmosphere. These TGA data reveal that the Fe_3O_4 loading in PVA-Fe_3O_4 is 20 wt.% with two-step degradation (one at 278 ºC for PVA and one at the onset of 460 ºC for Fe_3O_4) and SLGAPC loading in PVA-SLGAPC was 15 wt% with 2 step degradation (one at 278 ºC for PVA and one at the onset of 340 ºC for

SLGAPC). In the case of PVA-SLGAPC- Fe_3O_4 composite sample, Fe_3O_4 was 20 wt% and SLGAPC was 15 wt% with 3 step degradation (one at 278 ºC for PVA and at onset of 498 ºC for SLGAPC and one at the onset of 620 ºC for Fe_3O_4).

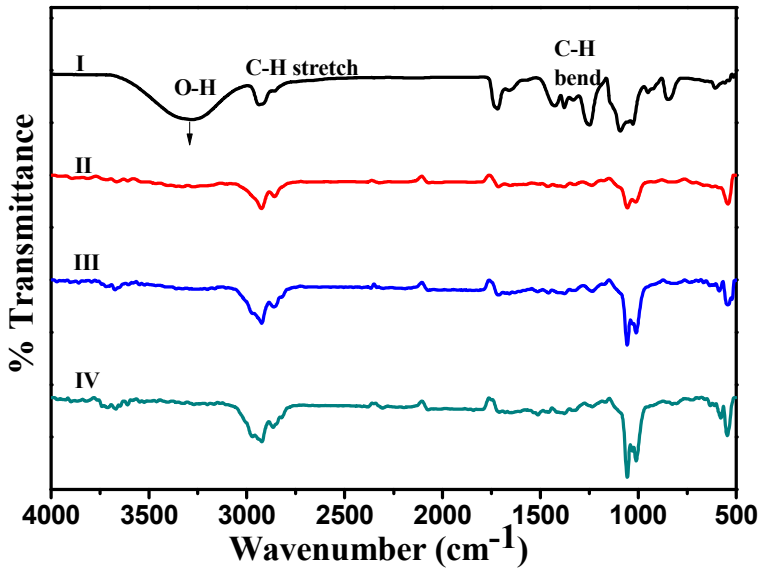

Figure 4: FTIR spectrum of I) PVA, II) PVA- Fe_3O_4, III) PVA-SLGAPC, IV) PVA-SLGAPC-Fe_3O_4 composites

FTIR analysis: Figure 4 shows the FTIR spectrum of I) PVA, II) PVA- Fe_3O_4, III) PVA-SLGAPC and IV) PVA-SLGAPC- Fe_3O_4. The salient signatures of PVA are seen in the composite. The characteristic signatures of hydrogen bonded (-OH) stretch bands at 3200-3570, and C=C band at 1649 cm^{-1}, [25] C-H stretch bands at 1373 and 1319 cm^{-1}, C-O bands at 1142 and 1088 cm^{-1}, [4] C-H bending bands at 842 cm^{-1} are observed in PVA film as well as in PVA composite films but with less intensity. In the composite samples, the bands at 2932 and 2864 cm^{-1} represents C-H stretching band and at 1716 cm^{-1} represents carbonyl C=O band and the additional peak of C-H stretching band at 2976 cm^{-1} in III & IV sample shows the characteristic presence of SLGAPC.[4, 25] These results suggest that the adsorption of Fe_3O_4 on the surface of SLGAPC conjugation with PVA occurs through O-H groups PVA and fillers.

Importantly, the SLGAPC is reported to be an extremely porous system which is rich in electrons[19] which could help improve the conductivity of the composite sample concomitantly. However, since SLGAPC is in the PVA matrix which has OH bonds at their edges, the conductivity may alter. Furthermore, the Fe_3O_4 molecules are also located in the composite matrix, which could induce a fine barrier region between the electrons (of SLGAPC) and the OH ions of PVA matrix, thereby forming localized capacitors. The results discussed further, clarify this issue.

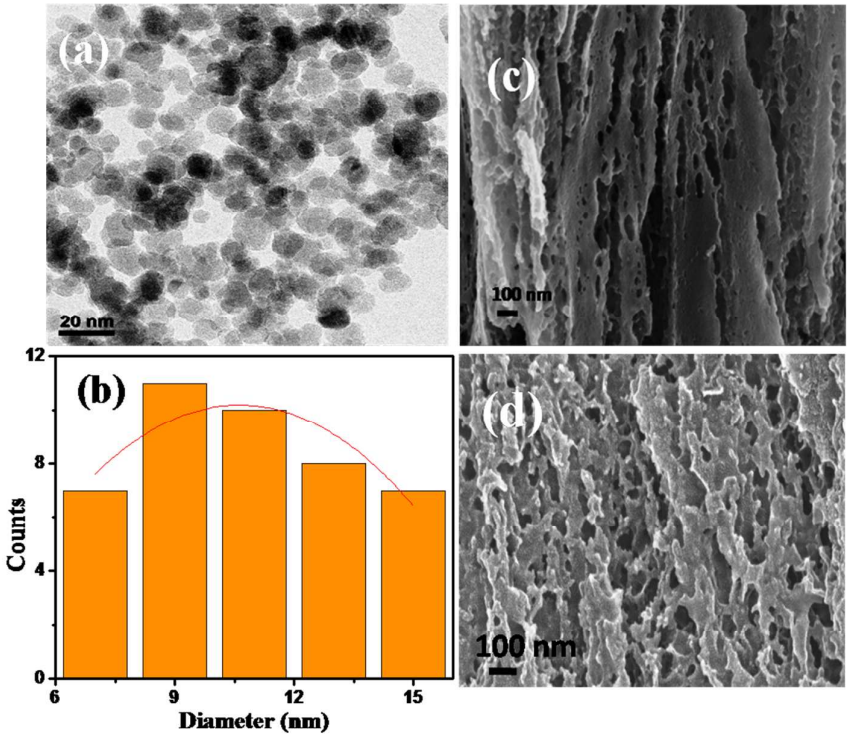

Figure 5 (i): (a), (b) are TEM and average size distribution of Fe_3O_4 nanoparticles, (c) and (d) FE-SEM images of SLGAPC and PVA-SLGAPC- Fe_3O_4 composites. The highlighted circles show presence of Fe_3O_4 nanoparticles in the composite.

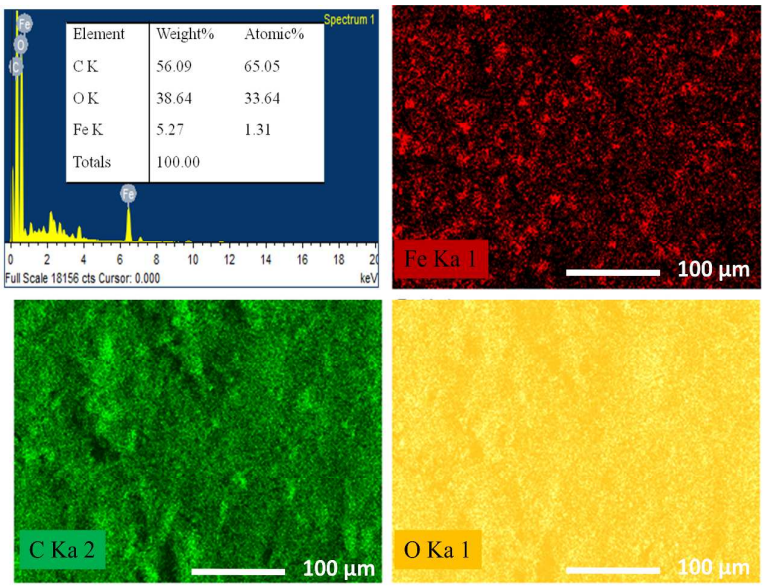

Figure 5 (ii): EDS of PVA-SLGAPC- Fe_3O_4 composite showing uniform dispersion of Fe, C and O in the three phase composite by elemental mapping.

Imaging: Figure 5 (i) shows the imaging data of the samples. Figure 5 (i) (a), (b) show the TEM image and size distribution of the Fe_3O_4 nanoparticles[20], which depicts particles of ~11 nm. Figure 5((i) c) shows FE-SEM image of SLGAPC material, which depicts the hexaporous nature of carbon structure[19]. Figure 5((i) d), shows the FE-SEM image of PVA-SLGAPC-Fe_3O_4, depicting the uniform distribution of Fe_3O_4 nanoparticles in the PVA-SLGAPC matrix. The composite was hence seen to be homogeneous and FTIR revealed that the iron oxide nanoparticles were embedded in the matrix of PVA and SLGAPC. Hence, mostly the free electrons of SLGAPC would be in close proximity to OH^- ions of PVA with metal oxide nanoparticle inclusions, thereby forming microcapacitors throughout the film.

Figure 5 (ii) shows EDS of PVA-SLGAPC- Fe_3O_4 composite with the distributions of Fe, C and O in terms of their elemental mapping. The quantitative estimate of the elements is also given in the inset of figure 5 (ii).

Dielectric properties at room temperature: The dielectric properties such as real part of permittivity (ε'), real part of conductivity (σ'), tangent loss (tanδ) and imaginary part of electric modulus (M'') of the composites were deduced from the measurement of capacitance and resistance of the samples using high-resolution Novocontrol broadband dielectric spectrometer. The composite films were given proper electric contact by quick drying silver paste and were placed between gold plated electrodes (dia. 20 mm).

Figure 6 shows the dielectric properties (ε', σ',tanδ and M'') as a function of frequency at room temperature. Figure 6(a) shows that with the inclusion of Fe_3O_4 in the PVA- SLGAPC system, the ε' is increased from 58 to 206 when compared to pure PVA film (ε'=12). This indicates two things: First is that SLGAPC itself shows a huge rise in the dielectric constant value to 58 (at 1 kHz), as compared to its other carbon-forms (such as CNTs, graphene, GO and so on).[7-12] This enhancement is mainly due to huge porosity (30±10 nm) in SLGAPC, as is reported earlier.[19] Secondly, in the presence of Fe_3O_4 in PVA-SLGAPC, ε' rises further to 206 which can be attributed to strong interfacial polarization leading to charge accumulation at the interfaces. The presence of these charges originates from the specimens preparation stage.

Figure 6 (b) shows an improvement in the conductivity (ac field) of PVA matrix upon Fe_3O_4 inclusion (from 7.4 x 10^{-10} S/cm for Fe_3O_4 to 1.0 x 10^{-9} S/cm). The composites PVA-SLGAPC and PVA-SLGAPC-Fe_3O_4 show the values 1.39 x 10^{-7} S/cm and 3.37 x 10^{-7} S/cm, respectively. This reflects an improvement in the capacitive performance of the composite, as compared to the original PVA as well as PVA-Fe_3O_4 counterparts. The conductivity, complex permittivity and tangent loss are given by the expressions:

$$\sigma^* = \sigma' - j\sigma'', \text{ where } \sigma' = \varepsilon_o \omega \varepsilon'' \quad (3)$$

$$\varepsilon^* = \varepsilon' - j\varepsilon'' \quad (4)$$

ε', ε'' are the real and imaginary parts of the complex permittivity, $\varepsilon_o = 8.85 \times 10^{-12}\ Fm^{-1}$

$$\tan\delta = \left(\frac{\varepsilon''}{\varepsilon'}\right) \quad 5$$

The composite samples thus show enhanced dielectric constant (ε') as compared to PVA and PVA- Fe_3O_4. As the frequency increased, the dielectric constant decreases rapidly upto 1 kHz and then decreases slowly, due to lack of adequate time to polarize the dipole/molecules. These high values can be attributed to the enhanced grain boundary effects, resulting in accumulation of charge carriers on the grain boundaries, thereby increasing the dielectric constant values.[15, 16 and 22]

Figure 6(c) reveals that inclusion of Fe_3O_4 in PVA matrix causes reduction of loss tangent (Tan δ) from 0.11 to 0.09 and in PVA-SLGAPC system from 4.42 to 2.75. This decrease in loss was due to the adsorption of Fe_3O_4 onto porous SLGAPC leading to strong interfacial polarization which causes charge accumulation at the interface, thus simultaneously showing enhancement in dielectric constant by ~4 times as compared to PVA-SLGAPC system; as tabulated in Table 1.

S.No.	Name of the sample	Dielectric constant real (ε') at 1.133 KHz	Conductivity (σ S/cm) at 1.133 KHz	Tangent Loss tan δ At 1.133 KHz	Electric modulus Imaginary (M") Peak Intensity at f_{max}
I	PVA	12	7.4×10^{-10}	0.11	0.023
II	PVA-20w% Fe3O4	18	1.0×10^{-9}	0.09	0.015
III	PVA-15w% SLGAPC	58	1.39×10^{-7}	4.42	0.014
IV	PVA-15w% SLGAPC-20w% Fe3O4	206	3.37×10^{-7}	2.75	0.004

Table 1: Dielectric properties ε', σ', Tan δ and M" of all samples at 1.133 KHz

As is seen from the Table 1, the response of PVA-SLGAPC is itself quite high, which further enhances with the formation of the three-phase composite. The dielectric loss tends to decrease as frequency increases, which is typically higher at low frequencies. This could be attributed to the induced relaxations due to the polarization effects caused by interfacial polarization and the dipole orientation or Debye losses.[22, 26]

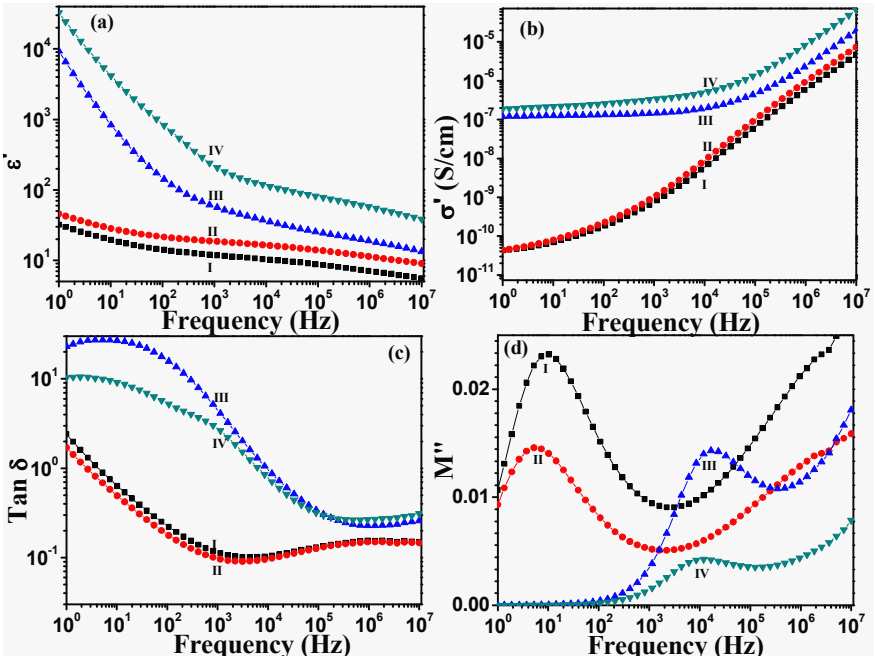

Figure 6: Frequency dependence of (a) dielectric permittivity (ε'), (b) conductivity (σ'), (c) loss tangent (Tan δ) and (d) imaginary part of electric modulus (M'') of the composites at room temperature.

Further to the study of the relaxation mechanism, the imaginary part of electric modulus formulation was used and is shown in Figure 6 (d). Electric modulus is expressed by the equation[26, 27]

$$M^* = \frac{1}{\varepsilon^*} = \frac{1}{\varepsilon' - j\varepsilon''} = \frac{\varepsilon'}{\varepsilon'^2 + \varepsilon''^2} + i\frac{\varepsilon''}{\varepsilon'^2 + \varepsilon''^2} = M' + iM'' \qquad 6$$

Addition of Fe_3O_4 in PVA as well as PVA-SLGAPC clearly shows that decrease in the intensity and shift in relaxation peaks is governed by Maxwell−Wagner−Sillars (MWS) polarization.[28]

As mentioned before, the SLGAPC network, when intercalated with PVA matrix, an array of distributed micro capacitors is formed with the metal oxide nanoparticle inclusions. Depending upon the spatial arrangement of Fe_3O_4 nanoparticles in the PVA-SLGAPC matrix, number of localized polarized sites would be created which can improve the dielectric constant dramatically. This particular property of the synergistic system of PVA, SLGAPC and Fe_3O_4 is the speciality of the formed composite which gives unusually high dielectric constants. To probe further into the nature of this system we measured the temperature dependent dielectric properties, discussed next.

Temperature dependent dielectric property study: Figure 7a) shows temperature evolution of real part of dielectric constant of IV) PVA-SLGAPC-Fe_3O_4 sample, as a function of frequency in the temperature range -30 ^oC (T_g -110 K) to 120 ^oC (T_g+40 K), where T_g is glass transition temperature around 80^oC for the PVA matrix. The temperature dependent dielectric constant data for the control samples, namely I) PVA, II) PVA-Fe_3O_4 and III) PVA-SLGAPC are shown in supporting information Figure S 2. The results suggest that with an increase in temperature the value of ε' increases continuously up to 80^oC and thereafter decreases. This is due the characteristic glass transition property of host polymer around 80^oC. Further, Figure 7b) shows the hysteresis of the dielectric constant with temperature (heating and cooling) for the IV) PVA-SLGAPC-Fe_3O_4 sample over the range -30 to 120^oC at 1 KHz. During the heating cycle the dielectric permittivity increases up to 120^oC, while in cooling cycle the dielectric response does not follow the same path, showing dielectric hysteresis which implies remnant polarization.[22, 29]

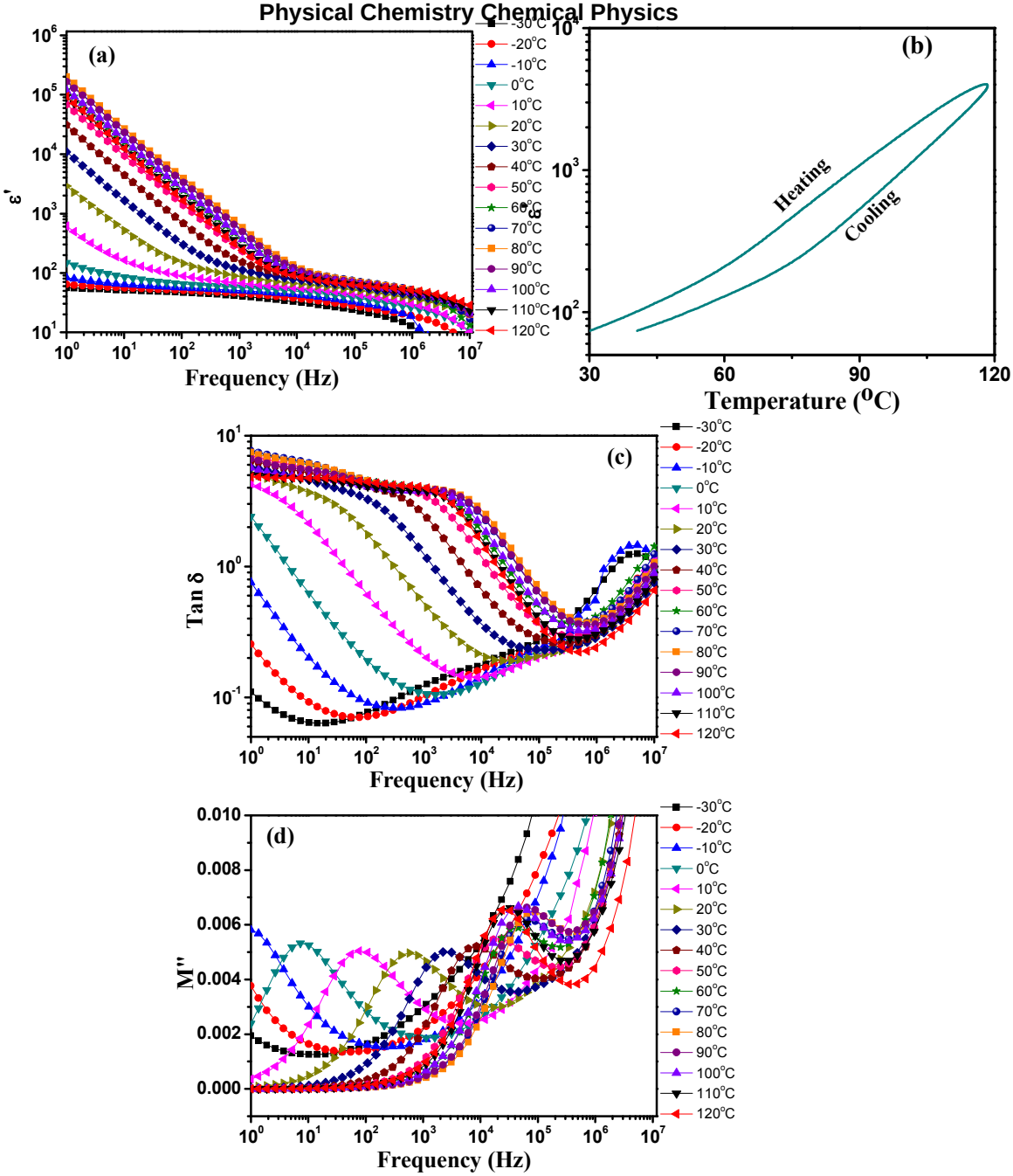

Figure 7: shows various data for sample IV. a) shows temperature dependence of ε′ w.r.t. frequency and b) shows thermal hysteresis of ε′ at 1 KHz. c) shows temperature dependence of Tan δ and d) shows temperature dependence of M″ as a function of frequency

Similar to dielectric permittivity behaviour, the temperature dependent loss tangent for the IV) PVA-SLGAPC-Fe_3O_4 composite is shown in Figure 7c) and the corresponding data for control samples, namely I) PVA, II) PVA-Fe_3O_4 and III) PVA-SLGAPC, are shown in

supporting information Figure S 3, lead to similar conclusions. The values of tangent loss decrease with frequency and shift towards higher frequency as temperature increases up to T_g and thereafter shift to lower frequency, showing typical Maxwell-Wagner-Sillars (MWS) relaxation processes.[28]

To understand the relaxation processes, temperature dependent imaginary part of electric modulus (M'') with frequency was also carried out and the results are shown Figure 7d) for IV) PVA-SLGAPC- Fe_3O_4 and the control sample data are shown in the supporting Figure S 4. In the temperature range from -30 ^oC to 80 ^oC as the temperature increases, the M'' relaxation peak shifts to higher frequency. The polymer chain motion increases due to increase in temperature and accumulation of free charges at the interface in the sample as well as increase in charge carrier mobility. As a result, the relaxation time decreases and there is a shift in relaxation peak towards higher frequency with increasing temperature. For above 80 ^oC, the M'' relaxation peak shifts towards lower side leading to composite polymer softening. All of these results are typical characteristics of MWS polarization relaxation and similar type relaxation is observed in other polymer composites.[1,28] These results thus confirm the localized interfacial polarization as well as the type of relaxation mechanism.

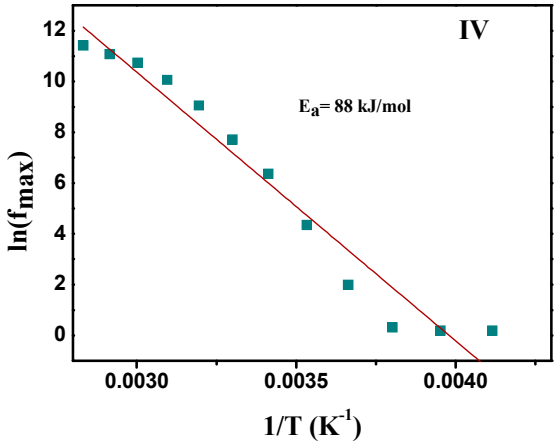

Figure 8: Arrhenius plot ln (f_{max}) vs 1/T for characteristic frequency of MWS polarization in IV) PVA-SLGAPC- Fe_3O_4 composite

Figure 8 shows the Arrhenius plot between ln of maximum frequency and reciprocal of temperature to understand MWS polarization relaxation processes in the IV) PVA-SLGAPC-Fe_3O_4 system and its counterparts shown in the supporting information Figure S 4, which are governed by power law expressed as

$$f = f_o \exp\left(-\frac{E_a}{kT}\right) \quad 7$$

Where f_o is the frequency at infinite temperature, k_B is the Boltzmann constant and E_a is the activation energy.[28] The values of the activation energy E_a of all the samples were calculated from the slope of the straight line plot of $\ln[f_{max}]$ with 1/T. The activation energy values of composite as well its counterparts are as shown in Table 2.

S.No.	Name of the sample	Activation energy (kJ/mol)
I	PVA	95.9
II	PVA-20w% Fe3O4	97.7
III	PVA-15w% SLGAPC	87.1
IV	PVA-15w% SLGAPC-20w% Fe_3O_4	88.0

Table 2: Activation energy values of the composites

From the Arrhenius plot, in the temperature range from -30 ^oC to 80 ^oC the activation energy of the IV sample is 88 kJ/mol, which suggests that the conduction processes is in between PVA and Fe_3O_4 modified SLGAPC are not prominent i.e. the barrier height is large, which suggests enhancement in the dielectric constant with reduced loss due to interfacial

polarization of adsorbed Fe_3O_4 on SLGAPC with the PVA matrix. Similar type of behaviour in activation energy was also observed in PVA-MWCNT composites, before.[30]

Therefore, we suggest that the interfacial polarization in adsorbed Fe_3O_4 on SLGAPC in PVA composites is contributing to the higher dielectric constant. The interfacial polarization is also known as a Maxwell−Wagner−Sillars (MWS) polarization, which originates from the blocked charge carriers at the interface between filler and matrix because of electrical conductivity differences between them.[28] The temperature dependent M" vs. frequency plot suggests that as the temperature increases, the relaxation peak increases towards higher value up to Tg (353 K) which shows the MWS polarization relaxation and above Tg the relaxation peak shows decrement in nature due to low values of activation energy. Similar type of relaxation behaviour was observed earlier.[22] However, the results in the reported cases do not show such a large change, as seen in the present case. The advantage of this work is not only in terms of higher achievable dielectric parameter values, but also the flexibility. Hence in this work a flexible material with superior dielectric response properties is designed and demonstrated which could find valuable use in capacitors as well as for EMI applications.

Electromagnetic interference (EMI) shielding application: Envisaging that the material designed in this work could be applicable in one of the most promising applications, namely EMI shielding, we subjected it to electromagnetic interference studies. Electromagnetic interference shielding properties of these composites of thickness 0.3 mm in X band (8.2-12.4 GHz) of dimensions 2.3×1.1 cm^2 were studied by measuring S-parameters through vector network analyzer, which are used in measuring shielding effectiveness (S.E) [31]

$S.E\ (dB) = -10 * log\ [\frac{P_I}{P_T}]$ Where P_I and P_T are Input and Transmit powers respectively. 8

$$S.E\ (dB) = S.E_R + S.E_A \quad 9$$

Where shielding effectiveness by reflection $S.E_R = -10 * \log(1 - R)$ and shielding effectiveness by absorption $S.E_A = -10 * \log\left[\frac{T}{(1-R)}\right]$; $R = |S_{11}|^2, T = |S_{21}|^2$,

S_{11} is represents the power received at antenna 1 relative to the power input to antenna 1 and S_{21} represents the power received at antenna 2 relative to the power input to antenna 1

Shielding effectiveness in terms of dielectric constant (ε), conductivity (σ') and permeability (μ') is

$S.E_R = -10 * log\ [\frac{\sigma'}{16\omega\mu'\varepsilon_0}]$ And $S.E_A = -10 * log\ [\frac{\sigma'\omega\mu'}{2}]^{\frac{1}{2}}$ where $\sigma' = \varepsilon_o\omega\varepsilon''$ 10

Where ω is the frequency, ε_o is the permittivity of free space = 8.854×10^{-12} F/m, ε'' is the imaginary part of complex dielectric permittivity.

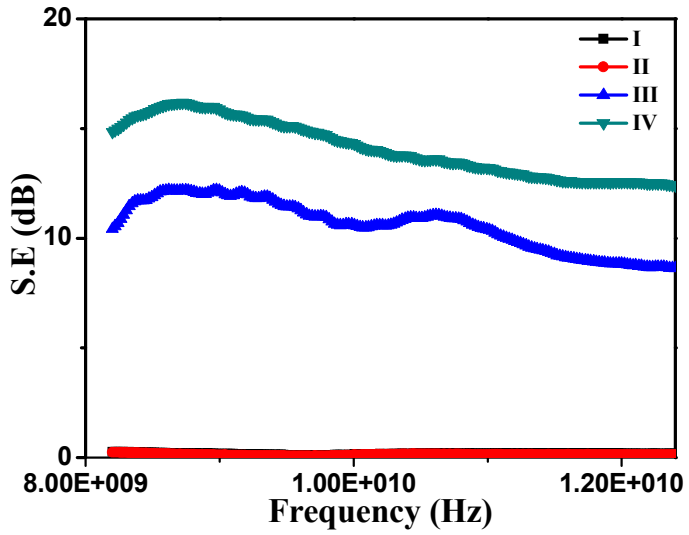

Figure 9: EMI shielding effectiveness (dB) of I) PVA, II) PVA-Fe_3O_4, III) PVA-SLGAPC, IV) PVA-SLGAPC- Fe_3O_4

Figure 9 shows the shielding effectiveness (S.E) versus frequency plot of the composite films having thickness 0.3 mm, in which the composite PVA-SLGAPC gives S.E of 10 dB whereas Fe_3O_4 nanoparticles included PVA-SLGAPC shows a S.E of 15 dB. S.E of 15 dB loss means

96.9% of power is getting shielded and only 3.1% is transmitting. This enhancement in S.E is due to high dielectric permittivity and conductivity of the three phase composite.

As mentioned before, there have been many reports on the use of complex composites to enhance the radio-frequency responses of these materials. The approaches have been of two types: use of non-conducting polymers and incorporating magnetic and conducting dopants therein; or using a conducting polymer and incorporating magnetic dopants. Both approaches have yielded enhanced of EMI properties. Saini et.al.[31] have studied improved EMI response of polyaniline (PANI) coated fabrics containing dielectric and magnetic nanoparticles. They have attributed their enhanced SE in Ku-band to the better matching of input impedance, reduction of skin depth, and additional dielectric and magnetic losses. Similar studies have been done by many groups using PANI, since it is a conducting polymer. In the efforts on nanocomposites in non-conductive matrix, the theory of percolation threshold is invoked, which talks about the conductive networks created by the filler content; which if exceed a certain critical value, (Percolation Threshold Value (PTV)), show enhanced properties.

For carbon-based system, mostly the reports have been with conducting carbon and use of magnetic fillers. For example, Shen et.al.[32] have reported specific shielding effectiveness 41.5 dB/(g/cm^3) for graphene:Fe_3O_4 and Ling et.al.[33] also reported specific shielding effectiveness of 17 - 44 dB/(g/cm^3) for PEI:graphene foam with thickness of 3 mm. However, owing to the SLGAPC system that has been used in this work, the S.E of 15 dB has been obtained for a extremely thin and flexible system of merely 0.3 mm. The corresponding specific S.E is 20 dB/(g/cm^3), which offers a good promise to the EMI domain researchers and application scientists, since the material would be much thinner, lightweight and with better properties. N. Yousefi et.al.[34] have reported fine work on aligned graphene sheets which offer high anisotropy of reduced graphene in polymer matrix. R. Kumar et.al.[35] recently reported

enhanced electromagnetic shielding effectiveness in their work with carbon foam embedded with Ni nanoparticles. They have mentioned that Ni nanoparticles embedded in the carbon material play an important role for improving the structure and electrical conductivity. The dispersion of Ni particles embedded in the polymer matrix was uniform and it improves absorption losses, provide higher surface; which further enhances the SE due to the absorption. The data show an increase in the imaginary permittivity and decreasing permittivity in carbon foam-Ni with frequency which has been ascribed to the decreasing capability of the dipoles to sustain the in-phase movement with speedily pulsating electric vector of the incident radiation. However, in these works the higher value of electrical conductivity is seen. The higher value of the imaginary permittivity may not store energy, but will be convert it into thermal energy inside the material, which attenuates the EM radiation. The carbon can easily dissipate the thermal energy due to its high value of thermal conductivity. In our case, the results are rather different. The electrical conductivity does not change much, In fact, considering the high conductivity values of SLGAPC, we did expect similar results. That also explained our originally high dielectric constant values for original SLGAPC itself. However, as seen from these studies on the composites formed, since the edges of carbon networks interact with PVA and because of the charge accumulation at Fe_3O_4 grains, the conductivity of the composite does not enhance much. But the system forms small capacitors throughout the film matrix, which not only enhances the dielectric constant values, but also shows extremely good shielding effectiveness. Hence interfacial polarization occurs in our heterogeneous materials due to the accumulation of charges at the interfaces and the formation of large dipoles. The three dimensional structures of SLGAPC, uniform dispersion of Fe_3O_4 nanoparticles in the PVA-SLGAPC matrix, specific interactions at the Fe_3O_4 grain boundaries; resulting in the superior dielectric properties; thereby generating a flexible and light weight EMI shielding material in the X-Band, is the novelty of this work.

CONCLUSION

Highly porous, flexible single layer grapheme assembled 3D conducting carbon is synthesised and used for form a three component composite with PVA and Fe_3O_4 nanoparticles fillers. The three phase, flexible composite films are seen to exhibit dramatic enhancement in the dielectric properties as compared to the separate components for their two phase composites. Adsorption and stability studies revealed the maximum adsorption limit of Fe_3O_4 nanofillers in porous SLGAPC is 20 wt%, suggesting saturation for further loading. Measurements reveal that the adsorption of Fe_3O_4 on PVA-SLGAPC generates interfacial polarization (MWS relaxation) that exhibits concomitant increase in the dielectric constant by a factor of 4 times and a decrease in the dielectric loss by a factor of 2, as compared to the PVA-SLGAPC composite without magnetic nanofillers. The structure, morphology, stability, optimal loading, dielectric hysteresis are studied in details. It is proposed that the adsorption of Fe_3O_4 on SLGAPC conjugated with PVA leading to substantial interaction between matrix and fillers, and enhances dielectric properties due to strong interfacial polarization. The modified three phase PVA-SLGAPC-Fe_3O_4 composite with enhanced dielectric properties shows more than 96.9% shielding efficiency in the X-Band of the electromagnetic spectrum exhibiting its promise for EMI shielding applications.

ACKNOWLEDGEMENT

Authors at DIAT acknowledge Dr Prahlada, former Vice Chancellor for support. Funding support of the "DIAT-DRDO Programme on Nanomaterial" and the DIAT-NCL collaboration by ERIPR, DRDO is thankfully acknowledged.

SUPPORTING INFORMATION (SI)

Additional information, such as temperature dependence of dielectric permittivity (ε') as a function of frequency of the I) PVA, II) PVA- Fe_3O_4 and III) PVA-SLGAPC samples is shown in Figure S 2. The temperature dependence of the loss tangent (Tan δ) as a function of frequency of the I) PVA, II) PVA- Fe_3O_4 and III) PVA-SLGAPC is shown in Figure S 3. The temperature dependence of imaginary part of electric modulus (M") as a function of frequency of the I) PVA, II) PVA- Fe_3O_4 and III) PVA-SLGAPC samples is shown in Figure S 4. The Arrhenius plots ln (f_{max}) vs 1/T for characteristic frequency of MWS polarization as a function of frequency for the cases of I) PVA, II) PVA- Fe_3O_4, III) PVA-SLGAPC and IV) PVA-SLGAPC- Fe_3O_4 composites are shown in Figure S 5. Shielding effectiveness (S.E) in terms of individual components of reflection and absorption of IV) PVA-SLGAPC- Fe_3O_4 hybrid composite film shown in Figure S 6 a) and thickness dependent (0.3-0.6 mm) S.E of IV) PVA-SLGAPC- Fe_3O_4 hybrid composite film has shown in Figure 6 b). This material is available free of charge via the internet at http://pubs.rsc.org.

AUTHOR INFORMATION

*Corresponding Authors:

[a]S. N. Kale
Email: sangeetakale2004@gmail.com,
[a]Department of Applied Physics, Defence Institute of Advanced Technology, Girinagar, Pune 411025, India.

[b]H. S. Panda
Email: himanshusp@diat.ac.in, hspanda3@gmail.com
[b]Department of Materials Engineering, Defence Institute of Advanced Technology, Girinagar, Pune 411025, India.
[c]S. B. Ogale
Email: sb.ogale@ncl.res.in
[c]National Chemical Laboratory, Homi Bhabha Road, Pashan, Pune 411008, India.

REFERENCES

(1) B. J.-P. Adohi and C. Brosseau, *J. Appl. Phys.,* 2009, **105**, 054108.

(2) M. P. Aji, S. Bijaksana and M. Abdullah, *ISRN Mater. Sci.,* 2012, **2012**, 1–7.

(3) A. Nigrawal and N. Chand, *Prog. Nanotechnol. Nanomater.,* 2013, **2**, 25–33.

(4) Z. Guo, D. Zhang, S. Wei, Z. Wang, A. B. Karki, Y. Li, P. Bernazzani, D. P. Young, J. A. Gomes, D. L. Cocke and T. C. Ho, *J. Nanoparticle Res.* 2009, **12**, 2415–2426.

(5) J. Belattar, M. P. F. Graça, L. C. Costa, M. E. Achour and C. Brosseau, *J. Appl. Phys.* 2010, **107**, 124111.

(6) A. Joshi, A. Bajaj, R. Sigh, P. S. Alegaonkar, K. Balasubramanian and S. Dattar, *Nanotechnology.* 2013, **24**, 455705.

(7) I. Tantis, G. C. Psarras and D. Tasis, *Express Polym. Lett.* 2012, **6**, 283–292.

(8) S. Stankovich, D. A. Dikin, G. H. B. Dommett, K. M. Kohlhaas, E. J. Zimney, E. A Stach, R. D. Piner, S. T. Nguyen and R. S. Ruoff, *Nature* 2006, **442**, 282–286.

(9) D. Galpaya, *Graphene* 2012, **01**, 30–49.

(10) S. G. Rathod, R. F. Bhajantri, V. Ravindrachary, P. K. Pujari, T. Sheela and J. Naik, *AIP Conf. Proc.* 2014, **1769**, 1769–1771.

(11) H. Kim, A. a. Abdala and C. W. Macosko, *Macromolecules*, 2010, **43**, 6515–6530.

(12) J. Liang, Y. Huang, L. Zhang, Y. Wang, Y. Ma, T. Cuo and Y. Chen, *Adv. Funct. Mater.*, 2009, **19**, 2297–2302.

(13) G. Zheng, J. Wu, W. Wang and C. Pan, *Carbon N. Y.* 2004, **42**, 2839–2847.

(14) S. Ansari and E. P. Giannelis, *J. Polym. Sci. part B Polym. Phys.* 2009, **47**, 888–897.

(15) G. C. Psarras, *J. Polym. Sci. part B Polym. Phys.* 2007, **45**, 2535–2545.

(16) G. C. Psarras, E. Manolakaki and G. M. Tsangaris, *Compos. Part A Appl. Sci. Manuf.*, 2003, **34**, 1187–1198.

(17) M. Londono, *Revi.EIA.Esc.Ing.Antioq* 2012, **18**, 105–114.

(18) J. Rault, R. Gref, Z. H. Ping, Q. T. Nguyen and J. Neel, *Polymer (Guildf).* 1995, **36**, 1655–1661.

(19) P. Yadav, A. Banerjee, S. Unni, J. Jog, S. Kurungot and S. Ogale, *ChemSusChem*, 2012, **5**, 2159–2164.

(20) R. Kitture, S. Ghosh, P. Kulkarni, X. L. Liu, D. Maity, S. I. Patil, D. Jun, Y. Dushing, S. L. Laware, B. a. Chopade and S. N. Kale, *J. Appl. Phys.*, 2012, **111**, 064702.

(21) H. Aono, H. Hirazawa, T. Naohara, T. Maehara, H. Kikkawa and Y. Watanabe, *Mater. Res. Bull.*, 2005, **40**, 1126–1135.

(22) A. Radhamanohar and H. S. Panda, *J. Phys. Chem. C* 2014**, 118**, 18868-18877.

(23) O. W. Guirguis and M. T. H. Moselhey, *Nat. Sci.* 2012, **4**, 57–67.

(24) A. S. Roy, S. Gupta, S. Sindhu, A. Parveen and P. C. Ramamurthy, *Compos. Part B* 2013, **47**, 314–319.

(25) E. F. Dos Reis, F. S. Campos, A. P. Lage, R. C. Leite, L. G. Heneine, W. L. Vasconcelos, Z. I. P. Lobato and H. S. Mansur, *Mater. Res.*, 2006, **9**, 185–191.

(26) C. V. Chanmal, *eXPRESS Polym. Lett.*, 2008, **2**, 294–301.

(27) G. M. Tsangaris, G. C. Psarras and N. Kouloumbi, *J. Mater. Sci.*, 1998, **33**, 2027–2037.

(28) W. Wu, X. Huang, S. Li, P. Jiang and T. Toshikatsu, *J. Phys. Chem. C*, 2012, **116**, 24887–24895.

(29) T. Vin, H. L. W. Chan, Y. Chen and C. L. Choy, *IEEE Transcations Dielectr. Electr. Insul.* 1996, **3**, 800–805.

(30) G. Chakraborty, A. K. Meikap, R. Babu and W. J. Blau, *Solid State Commun.*, 2011, **151**, 754–758.

(31) P. Saini, V. Choudhary, N. Vijayan and R. K. Kotnala, *J. Phys. Chem. C* 2012, **116**, 13402–13415.

(32) B. Shen, W. Zhai, M. Tao, J. Ling and W. Zheng, *ACS Appl. Mater. Interfaces.* 2013, **5**, 11383−11391.

(33) J. Ling, W. Zhai, W. Feng, B. Shen, J. Zhang and W. Zheng, *ACS Appl. Mater. Interfaces.* 2013, **5**, 2677−2684.

(34) N. Yousefi, X. Sun, X. Lin, X. Shen, J. Jia, B. Zhang, B. Tang, M. Chan and J. Kim, *Adv. Mater.* 2014, **26**, 5480–5487.

(35) R. Kumar, S. Kumari and S.R. Dhakate, *Appl Nanosci* 2014, (DOI 10.1007/s13204-014-0349-7)

Table of Contents Graphic: